SCANNING VOL. 33, 78–81 (2011)

Investigation of Tibetian Plateau Varnish: New Findings at the Nanoscale Using Focused Ion Beam and Transmission Electron Microscopy Techniques

KURT A. LANGWORTHY[1], DAVID H. KRINSLEY[2], AND RONALD I. DORN[3]

[1]CAMCOR, University of Oregon, Eugene, Oregon
[2]Department of Geological Sciences, University of Oregon, Eugene, Oregon
[3]School of Geographical Sciences and Urban Planning, Arizona State University, Tempe, Arizona

Summary: Dual-beam focused ion beam microscopy (FIB/SEM) preparation of rock varnish for high-resolution transmission electron microscopy (HR-TEM) has enabled us to characterize unreported nanostructures. Fossils, unreported textures, and compositional variability were observed at the nanoscale. These techniques could provide a method for studying ancient terrestrial and extra-terrestrial environments to better understand geological processes at the nanoscale. SCANNING 33: 78–81, 2011. © 2011 Wiley Periodicals, Inc.

Key words: geology, FIB, STEM, EDS, Tibet, nanoscale

Introduction

Rock varnish is a coating of clay minerals, Fe-Mn oxyhydroxides, trace, and minor elements that cover rock surfaces exposed to the atmosphere in many varied Earth environments (Potter and Rossman, '77; Jones '91). The investigation of rock coatings and varnish has progressed considerably through the use of scanning electron microscopes (SEM) in back-scattered (BSE) and secondary electron (SE) modes (Krinsley *et al.*, '90). Characterization using SEM techniques are typically limited by instrument image resolution and energy dispersive x-ray spectrometer (EDS) resolution, influenced by both detector resolution (eV) and x-ray scattering into specimens (Goldstein *et al.*, 2003). Compositional and physical variation have been observed at the micron level (Dorn, '98); we were interested in determining if further variation existed at the nanoscale. To better study intrinsic features and chemical composition of varnish at the nanoscale, high-resolution transmission electron microscopy (HR-TEM) was used. Preparing HR-TEM samples with a dual-beam focused ion beam microscope (DB-FIB) allows for site-specific investigations to be performed at much higher resolution than conventional SEM techniques allow (Heaney *et al.*, 2001; Garvie et al., 2008; Wirth, 2009).

Interest in natural rock coatings has recently increased by the discovery of similar materials on Mars (DeGregorio, 2002; Murchie *et al.*, 2004; Spilde et al., 2008). Thus, it may be appropriate to investigate the physical attributes and the chemical composition of small particles found in rock coatings on Earth to better understand Martian environmental conditions leading to varnish formation. Environmental conditions of the Tibetian Plateau are thought to be somewhat analogous to Mars (Krinsley *et al.*, 2009). This article reports considerable variation in composition and physical features at the nanometer level within varnish coatings from the Tibetian Plateau. We present our experiences with the TEM, including sample preparation, the use of various imaging modes, and our compositional findings.

Materials and Methods

Samples of rock varnish were prepared by cutting a rock chip from a larger sample, placing the chip in a one-inch lexan ring, then backfilling the ring with liquid epoxy to prevent the sample from crumbling. Rock samples with varying feature heights are

Address for reprints: Kurt A. Langworthy, CAMCOR, University of Oregon, Eugene, OR 97403-1241
E-mail: klangwor@uoregon.edu

Received 3 December 2010; Accepted with revision 8 February 2011

DOI 10.1002/sca.20226
Published online 4 March 2011 in Wiley Online Library (wileyonlinelibrary.com)

challenging to manipulate at short working distances in electron microscopes. To prevent accidental damage to the microscope's pole piece, the plug/sample was ground flat and polished until it was highly reflective. It was examined and photographed with a reflected light microscope in order to locate initial areas of interest. After light microscopy, the plug was examined in both BSE (Fig. 1) and SE modes, using a FEI Helios DB-FIB microscope. BSE imaging was used to locate analysis sites by utilizing atomic number contrast exhibited by variability in geological minerals (Krinsley, '98). After locating the areas, a thin layer of Pt metal was deposited with the DB-FIB to help protect the outermost surface from ion beam damage, and decrease curtaining effects often observed while milling dissimilar materials (Formanek and Bugiel, 2006). Ion beam milling, after Pt deposition, was performed on each side of the analysis site to create a 15-μ wide, 5-μ deep specimen for cross-section lift-out to be analyzed in a HR-TEM. The cross-section was lifted out of the bulk specimen *in situ* with the use of an Omniprobe micromanipulator and attached to a copper TEM grid using a platinum gas precursor. We ion thinned and polished our specimens at low beam currents; this allowed us to carefully monitor the thickness of our specimens, as well as to minimize accidental beam damage. The cross-sections were further thinned and ion polished at 5 kV, 16 pA using the DB-FIB to produce approximately 100-nm thick specimens for HR-TEM analysis. Despite our careful approach to ion milling, some areas of our cross-sections were observed to deteriorate during thinning, making it difficult to preserve entire specimens. HR-TEM analysis was performed with an image-corrected, FEI Titan transmission electron microscope. Images of samples were obtained in bright-field and dark-field STEM (scanning-transmission electron microscopy) mode. Although some features could only be seen in bright field, STEM mode provided extremely good contrast in comparison, and was highly useful for phase/grain identification. Compositional analysis was performed in STEM mode with an EDAX EDS detector at 300 kV with moderate beam current and a 4-sec dwell time per analysis spot.

Discussion and Conclusions

High-resolution transmission electron microscopy was used to characterize Tibetian Plateau rock varnish at the nanometer level. The cross-sections analyzed were extracted from an area at the edge of the varnish (Figs. 1 and 2). As seen in Figure 1 (with SEM in BSE mode), atmospheric grains (fall-out) appear to be absorbed into some portions of the varnish layers. Bright-field imaging, dark-field STEM imaging, and EDS analyses were performed in the HR-TEM to characterize the cross-sections. Bright-field imaging showed lattice patterns to be present at many locations (Fig. 3), indicating that some regions, structures, and particles were crystalline. The d-spacing of the lattices can be further examined to identify crystal structure and size of unit cell (Jackson, '91).

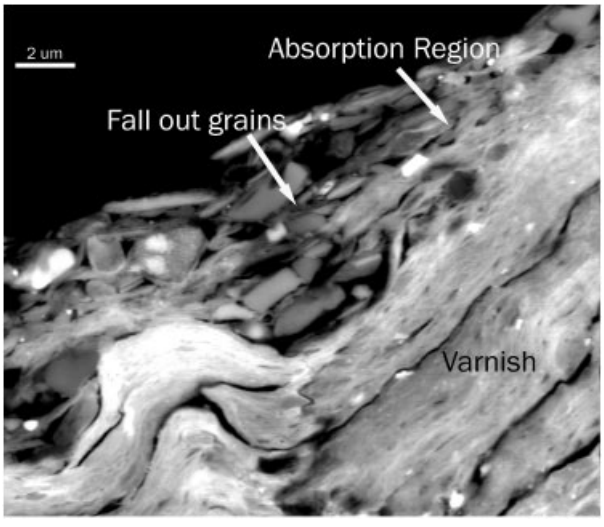

Fig 1. Backscatter SEM image of varnish boundary, showing absorption of fall-out grains into varnish layers. SEM, scanning electron microscope.

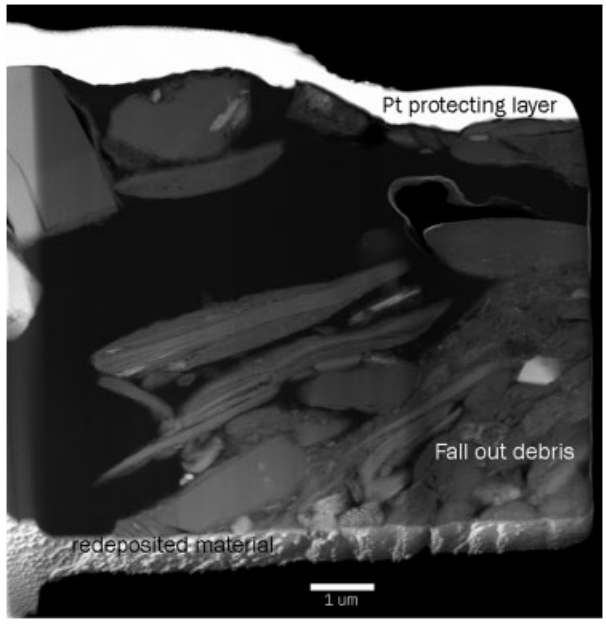

Fig 2. Low-magnification STEM image of TEM cross-section, prepared using DB-FIB lift-out technique. STEM, scanning-transmission electron microscopy; DB-FIB, dual-beam focused ion beam microscope.

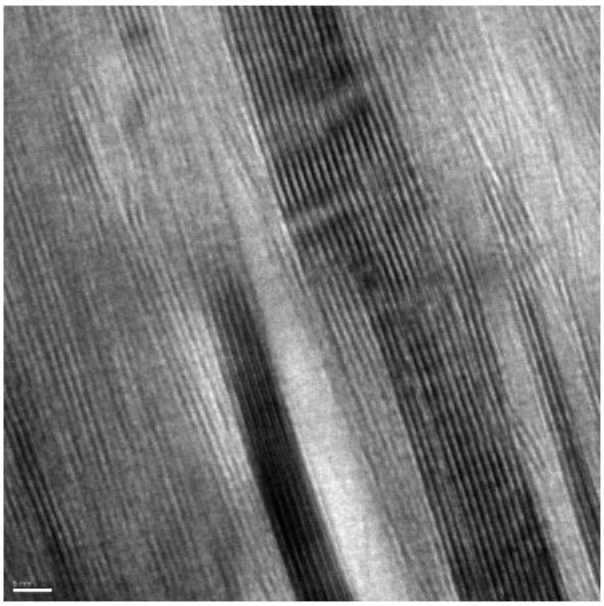

Fig 3. High-resolution TEM image showing an example of lattice structures present in Tibetian Plateau varnish. TEM, transmission electron microscope.

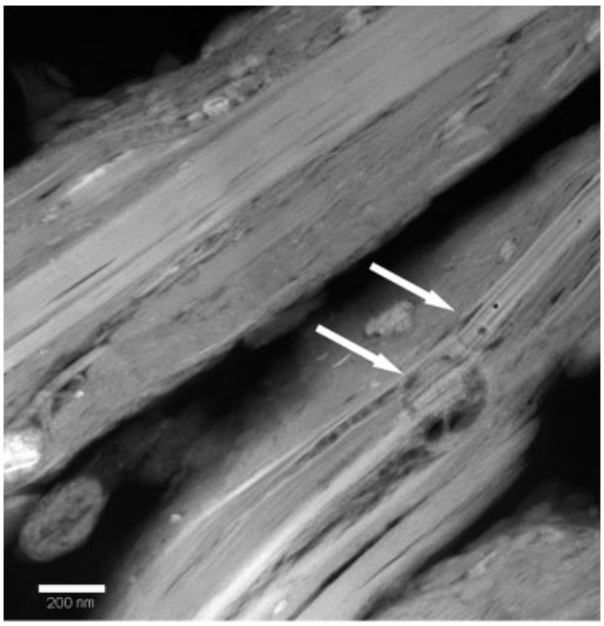

Fig 4. Putative fossils in Tibetian Plateau varnish, observed in HAADF STEM mode. HAADF, high-angle annular dark-field; STEM, scanning-transmission electron microscope.

High-angle annular dark-field (HAADF) STEM mode allowed us to image the cross-sections with high contrast, primarily attributed to atomic number differences (Goldstein *et al*., 2003). During STEM mode analysis, we observed several structures, including what appeared to be fossils (Fig. 4), as well as SiO_x nanoparticles contained within larger grains. The SiO_x containing regions may be associated with various stages of quartz formation or

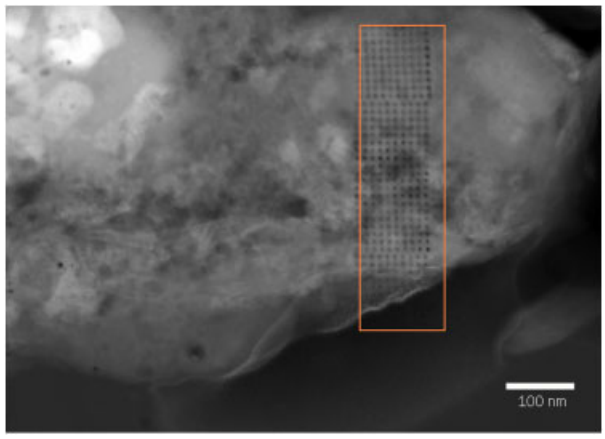

Fig 5. Beam-damage observed in grains during EDS analysis, displaying specific analysis points. EDS, energy dispersive x-ray spectrometer.

break down (Langworthy *et al*., 2010). The putative fossils seen were found in different stages of preservation. Many were approximately spherical in appearance, containing internal features that resemble structures seen in some modern bacteria (Oh *et al*., 2005; Edgar *et al*., 2006). The most visible fossils ranged from 70 to 220 nm in diameter (Fig. 4). Using EDS, we observed phosphorus counts in several regions of our cross-section. Phosphorus occurred in many of the visible fossil structures and in some regions around faintly visible fossils. Phosphorus occurrence in regions without visible fossils may suggest regions where extensive recrystallization occurred.

During EDS acquisition, we noticed our sample had been damaged by the electron beam (Fig. 5). The damage was associated with the thinness of the cross-section, which was approximately 100 nm. The damage was observed as a series of dots over the analysis region, indicating where each EDS spectrum had been acquired. The analysis region was 100 nm $\times$ 300 nm, containing 300 EDS analysis points, spaced 10 nm apart. Our analyses were duplicated to account for possible beam drift. As the beam penetrated/damaged the specimen, x-ray counts were observed to decrease. Though despite the loss of x-ray counts, the small excitation volume associated with the thin sample allowed us to observe compositional differences at the 10-nm scale (Fig. 6). Analysis over this region took approximately 20 min to complete. The x-ray excitation region of each spot was calculated with the Monte-Carlo simulation to be less than 10 nm (Goldstein *et al*., 2003).

The creation of thin TEM samples produced using DB-FIB microscopes make it possible to study structures at the nanoscale and aid in the characterization of rock properties at the submicron scale. Collecting data on natural rock coatings and

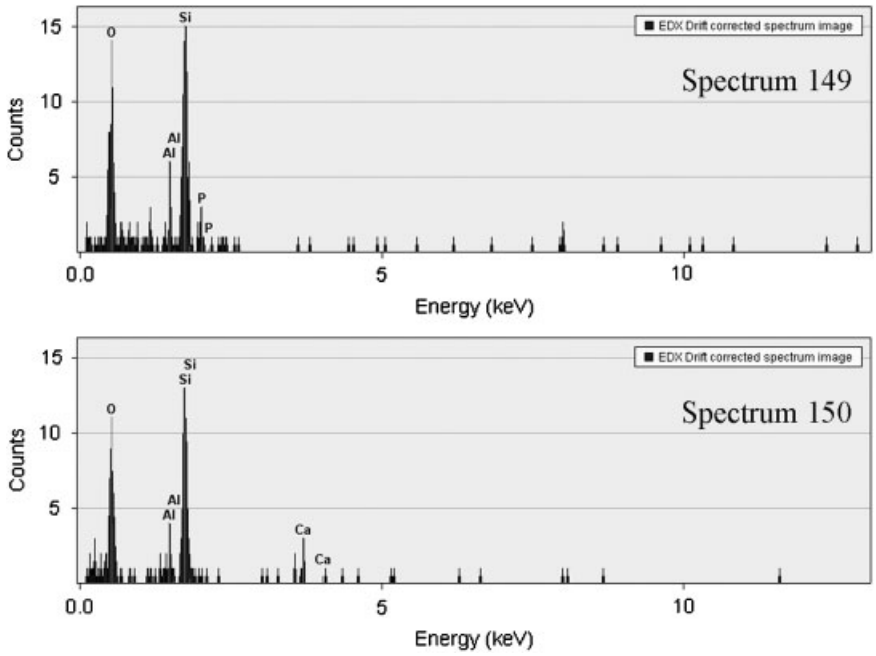

Fig 6. EDS spectra taken in sequence, 10 nm apart, illustrating compositional variability at the nanometer scale in Tibetian Plateau grains. EDS, energy dispersive x-ray spectrometer.

other geological specimens at high resolution could provide information about ancient organisms, ancient climates, as well as compositional and physical changes in rock coatings.

References

DeGregorio B. 2002. Rock varnish as a habitat for extant life on mars: instruments, methods and missions for astrobiology IV. In: Hoover RB *et al*., editors. Proceedings of the SPIE International Society on Optical Engineering, v. 4995. p 120–130.

Dorn R. 1998. Rock coatings. Amsterdam: Elsevier.

Edgar R, Michael McKinstry M, Hwang J, Oppenheim AB, Fekete RA, Giulian G, Merril C, Nagashima K, Adhya S. 2006. High-sensitivity bacterial detection using biotin-tagged phage and quantum-dot nanocomplexes. Proc Natl Acad Sci USA 103:4841–4845.

Formanek P, Bugiel E. 2006. Specimen preparation for electron holography of semiconductor devices. Ultramicroscopy 106:365–375.

Garvie LAJ, Burt DM, Buseck PR. 2008. Nanometer scale complexity, growth and diagenesis in desert varnish. Geology 36:215–218.

Goldstein J, Newbury D, Joy D, Lyman C, Echlin P, Lifshin E, Sawyer L, Michael J. 2003. Scanning electron microscopy and X-ray microanalysis. New York: Kluwer Academic/Plenum Publishers.

Heaney P, Vicenzi E, Giannuzzi L. 2001. Focused ion beam milling: a method of site-specific sample extraction for microanalysis of earth and planetary materials. Am Mineral 85:1094–1099.

Jackson AG. 1991. Handbook of crystallography for electron microscopists and others. Berlin: Springer. p 210.

Jones CE. 1991. Characteristics and origin of rock varnish from the hyperarid coastal deserts of Northern Peru. Quat Res 35:116–129.

Krinsley D. 1998. Models of rock varnish formation constrained by high resolution transmission electron microscopy. Sedimentology 45:711–725.

Krinsley D, Dorn R, Anderson S. 1990. Factors that interfere with the dating of rock varnish. Phys Geogr 11: 97–119.

Krinsley D, Dorn R, DiGregorio B. 2009. Astrobiology implications of rock varnish in Tibet. Astrobiology 9: 551–562.

Langworthy K, Krinsley D, Dorn R. 2010. High resolution transmission electron microscopy evaluation of silica glaze reveals new textures. Earth Surf Processes Landforms 35:615–1620.

Murchie S, Barnouin-Tha O, Barnoiun K, Bishop J, Johnson J, McSween H, Morris R. 2004. Old desert coatings and young breccias at the mars pathfinder landing sites. 35th Lunar and Planetary Science Conference, Lunar and Planetary Science Institute, Houston, TX. Abstract 1740.

Oh JD, Karam S, Gordon J, Falkow S. 2005. Intracellular *Helicobacter pylori* in gastric epithelial progenitors. Proc Natl Acad Sci USA 102:5186–5191.

Potter RM, Rossman GR. 1977. Desert varnish: the importance of clay minerals. Science 196:1446–1448.

Spilde MN, Boston PJ, Northrup DE, Odenbach KJ. 2008. Rock coatings: potential biogenic indicators. Ground truth from mars: science payoff from a sample return mission, Lunar and Planetary Institute, Houston, TX. Abstract 4045.

Wirth R. 2009. Focus ion beam (FIB) combined with SEM and TEM: advances analytical tools for studies of chemical composition, microstructure and crystal structure in geomaterials on a nanometre scale. Chem Geol 261: 217–229.